Synthesis, Characterization, X-Ray Diffraction Analysis of A Tridentate Schiff Base Ligand and Its Complexes with Co(II), Fe(II), Pd(II) and Ru(II): Bioactivity Studies

Buldurun, Kenan*[+]

Department of Food Processing, Vocational School of Technical Sciences, Muş Alparslan University, 49250 Muş, TURKEY

Turan, Nevin

Department of Chemistry, Faculty of Arts and Sciences, Muş Alparslan University, 49250 Muş, TURKEY

Savci, Ahmet; Alan, Yusuf

Department of Molecular Biology and Genetics, Faculty of Arts and Sciences, Muş Alparslan University, 49250 Muş, TURKEY

Colak, Naki

Department of Chemistry, Faculty of Arts and Sciences, Hitit University, 19100 Çorum, TURKEY

ABSTRACT: *This study reports the synthesis of Co(II), Fe(II), Pd(II), and Ru(II) complexes with Schiff base obtained by the condensation of 2-amino-methyl-4,5,6,7-tetrahydrothieno[2,3-c]pyridine-3-carboxylate with salicylaldehyde. The characterization of the ligand and its complexes was arranged and studied by FT-IR, UV-Vis., ^{1}H, and ^{13}C NMR, microanalyses (C, H, N, S), X-Ray Diffraction (XRD) analysis, magnetic susceptibility, mass spectra, and ThermoGravimetry Analysis (TGA) and further screened for antimicrobial, antioxidant, and antiradical activities. The antioxidant activity of the ligand and its metal complexes was examined by using different methods including the total antioxidant activity method, total reduction method, and DPPH. The antimicrobial activities of Schiff base and metal complexes were investigated on bacterial and fungal strains. DNA cleavage experiments of metal complexes with supercoiled pBR322 DNA were detected by gel electrophoresis in the being of H_2O_2.*

KEYWORDS: *DNA cleavage; Antimicrobial; Antioxidant; X-ray diffraction analysis; Schiff base; Metal complexes.*

***** *To whom correspondence should be addressed.*
+ E-mail: k.buldurun@alparslan.edu.tr
1021-9986/2022/8/2635-2649 15/$/6.05

INTRODUCTION

Schiff bases are compounds that contain azomethine (C=N) structure obtained from the condensation of ketones or aldehydes having the carbonyl (C=O) group and primary amines having amine (NH_2) groups [1,2]. Thanks to the easy adjustment of their molecular structures and electronic properties, and their inert properties against air and moisture, by using the Schiff bases and many of the transition metals, new stable complexes can be formed easily [3]. Recently, many different compounds having the Schiff base structure, due to their use in a variety of areas, have attracted the attention of scientists who study on synthesis and characterization of compounds. The ease of preparation of transition metal complexes obtained from Schiff base ligands, the presence of low-cost raw materials, the formation of stable and chelated coordination complexes in most transition metal complexes, and having a rich coordination step have led them to be preferred material in the fields of organic chemistry, inorganic chemistry, and biochemistry [4-7]. Schiff bases including salicylaldehyde and *p*-aminophenol are a few examples of these complexes and these Schiff bases, due to a lot of oxygen, nitrogen, and donor atoms, have got much different coordination modes [8]. Schiff bases and their transition metal complexes exhibit biological activities such as antimicrobial, analgesic, antioxidant, anti-inflammatory, and antiviral, and they are also known to be the leading actors in the catalytic field [9-11]. Furthermore, in addition to all these properties, these complexes have been reported to be examined in terms of synthetic flexibility, selectivity, sensitivity to various organisms, and catalytic activity in chemical and photochemical reactions [12,13]. Many studies carried out on the metal complexes have reported that these complexes exhibit superior properties in various fields, having significant value in the development of a country, such as electrochemistry, analytical chemistry, food, pesticides and dye industries, pharmaceutical chemistry, molecular electronics, and information processing and optical memory devices [14-21].

Schiff bases with donors (N, O, S, etc.) have structural similarities with neutral biological systems, and due to the presence of the imine group is utilized in elucidating the mechanism of transformation of insemination reaction in biological systems [22]. One of the important exogenous antioxidants is Schiff bases, which have significant biological and chemical importance because of their azomethine/imine (-C=N-) bonds in their structures. The great interest in this field has focused on the complexes formed by Schiff bases and their transition metal ions because of the nitrogen and oxygen-giving atoms in the molecular structure of these ligands. Schiff bases, which also include halogen groups, and their metal complexes, have been the focus of special interest in their antimicrobial properties. It was reported that the compounds that include one or more nitrogen atoms in the aromatic ring have biological activities, such as being antitumor, antioxidant, antibacterial, and antifungal [23]. Metal-based medications have gained a lot of importance in the medical field in recent years, and are used as medicine for the treatment of diabetes, cancer, and anti-inflammatory and cardiovascular diseases. Some of the Schiff bases and their transition metal complexes are also used as bactericidal, fungicidal, anti-tuberculosis, and antiviral agents [24-28].

Deoxyribonucleic acid (DNA) is a very significant genetic molecule in living things. DNA is the main molecular target for most drugs used to fight cancer. Schiff bases containing aromatic moieties and transition metal complexes have been extensively investigated by many scientists with their strong interactions with DNA, interfering or surface joining, and potential DNA cleavage activities. As a result, over the last decade, DNA degradation research has been studied with great interest by biologists and chemists. Numerous transition metal complexes that cleave DNA under physiological conditions are developed as an artificial nucleases. The structure of ligands and metals will lead the way in the design of complexes, and new drugs. Moreover, it has a key role in their interaction with the DNA molecule, which helps to develop new, selective, and effective DNA recognition and separation agents. Numerous transition metal complexes have been discovered that influence DNA cleavage due to their redox properties [29,30].

In this study, the synthesis of Co(II), Fe(II), Ru(II), and Pd(II) complexes with new Schiff base ligand and their structures using various spectroscopic methods were clarified. In addition, the study of DNA interaction with the biological properties of all compounds was presented. This was the first study to synthesize, characterize and investigate the properties of this ligand and its metal complexes.

EXPERIMENTAL SECTION

Materials and methods

All the chemicals and solvents (95-99% purity) used in the present work were purchased from Merck or Sigma-Aldrich and used without further purification. 2-amino-methyl-4,5,6,7-tetrahydrothieno[2,3-*c*]pyridine-3-carboxylate was synthesized using a similar method described in a previous paper [31]. Reference antibiotic discs were attained from Oxoid, Thermo Fisher Scientific (Wade Road, Basingstoke and Hampshire RG24 8PW, UK). Super wound *p*BR322 DNA was purchased from Thermo Scientific and stored at -20 °C. Double distilled water was used to prepare all buffer solutions for DNA binding studies. FT-IR spectra were measured as pellets using KBr on a Perkin Elmer 65 spectrometer. The proton (^{1}H-NMR) and carbon (^{13}C-NMR) NMR spectra were performed by Bruker GmbH DPX-400 MHz FT spectrometer. The electronic spectra of all the compounds were recorded on Shimadzu 1800 spectrophotometer using EtOH as the solvent in the range of 200-800 nm. Mass spectra were recorded *via* an AGILENT 1100 MSD spectrophotometer. Microanalysis was recorded on a LECO 932 CHNS analyzer. Magnetic sensitivity measurements were recorded using Hg[Co(SCN)$_4$] calibrated through Gouy balance. UltimaIV X-ray diffractometer by Rigaku (CuKα=1.540562 A°) was performed by the crystal properties of the complexes. Thermogravimetric analysis (TGA) was measured through a Perkin Elmer Pyres Diamond TG/DTA at a heating rate of 10 °C/min.

Synthesis and characterization of Schiff base ligand ((E)-methyl 2-(2-hydroxybenzylideneamino)-6-methyl-4,5,6,7-tetrahydrothieno[2,3-c]pyridine-3-carboxylate)

The Schiff base ligand was synthesized using 1 g (4.42 mmol) amine compound (2-amino-methyl-4,5,6,7-tetrahydrothieno[2,3-*c*]pyridine-3-carboxylate) dissolved in 10 mL ethanol and 0.46 mL (4.42 mmol) salicylaldehyde dissolved in 10 mL ethanol. The reaction mixture was heated for 3 h. The obtained pale yellow product was separated by filtration, washed with ethanol several times, and dried under in vacuum. The product was recrystallized with aqueous methanol and chloroform (1/2) mixture.

Schiff base: Yield: 90%; m.p.: 132 °C; Anal. Calc. for ($C_{17}H_{18}N_2O_3S$) (FW: 330.23 g/mol) (%): C 61.80, H 5.44, N 8.47, S 9.70. Found: C 61.80, H 5.47, N 8.48, S 9.71; FT-IR (KBr, cm^{-1}): 3434-3385, 3050, 2941, 2850, 1700, 1601, 1561, 1377, 1221, 750; ^{1}H-NMR (400 MHz, $CDCl_3$, δ, ppm):12.83 (s, H, OH), 8.44 (s, H, CH=N), 7.30-6.85 (m, 4H, Ar.-H), 3.86 (s, 3H, -OC=O-CH_3), 3.49-2.64 (m, 6H, CH_2), 2.41 (s, 3H, N-CH_3); ^{13}C-NMR (100 MHz, $CDCl_3$, δ, ppm): 163.54 (C=O), 159.27 (CH=N), 153.66 (C-OH), 134.46-132.08 ($C_{2\text{-thiophene}}$), 128.72-117.61 ($C_{1\text{-benzene}}$), 14.29, 26.78, 60.99 ($C_{piperidine}$), 51.55 (-OC=O-CH_3), 45.52 (N-CH_3); UV-vis (λ_{max}, nm): 212, 260, 314; Mass spectra: *m/z* 330.37 (calcd.), 331.37 (found) [M]$^+$.

Synthesis and characterization of Co(II), Fe(II), Pd(II) and Ru(II) complexes

15 mL hot ethanol of 0.19 g (0.9 mmol) of $FeCl_2{\cdot}4H_2O$ and 0.23 g (0.9 mmol) of $CoCl_2{\cdot}6H_2O$ was added dropwise to 15 mL hot ethanol 0.33g (1.0 mmol) Schiff base ligand solution and the reaction mixture was refluxed at 80 °C with stirring for 8 h. For the $PdCl_2(CH_3CN)_2$, 0.26 g (1.0 mmol), and [$RuCl_2$(*p*-cymene)]$_2$, 0.31 g (0.5 mmol), salts were used in toluene for 4 h after completion of the reaction and the obtained solid product was filtered off. The product was washed several times with diethyl ether and crystallized from the methanol/dichloromethane (1/3) mixture. The product obtained was recrystallized twice with aqueous ethanol and chloroform. The synthesis scheme of ligand and its metal complexes was shown in Scheme 1.

[$FeL_2(H_2O)_2$]·H_2O: Yield: 84%; m.p.: 300-306 °C; FW: 768.30 g/mol; FT-IR (KBr, cm^{-1}): 3555-3476, 3051, 2971, 2734, 1702, 1610, 1571, 1535, 1374, 1207, 751, 580, 522, 491, 457; Anal. calc. for ($C_{34}H_{40}FeN_4O_9S_2$): C 53.14, H 5.20, N 7.28, S 8.34; Found: C 53.14, H 5.20, N 7.30, S 8.38; UV-vis bands (λ_{max}, nm): 205, 269, 398, 439, 530, 640; Mass spectra: m/z 771.30 (calcd.), 769.93 (found) [M-2H]$^-$; Color: Black.

[RuCl(*p*-cymene)L]·$2H_2O$: Yield: 82%; m.p.: 200 °C; FW: 635.85 g/mol; FT-IR (KBr, cm^{-1}): 3434, 3055, 2959, 2869, 1702, 1609, 1567, 1522, 1380, 1202, 751, 548, 525, 459, 469; ^{1}H-NMR (400 MHz, $CDCl_3$, δ, ppm): 8.77 (s, H, CH=N), 7.45-6.92 (m, 8H, Ar-H), 3.90 (s, 3H, -OC=O-CH_3), 3.64-2.70 (m, 6H, CH_2), 2.26 (s, 3H, N-CH_3), 2.83-2.79 (m, 1H, CH of *p*-cymene moiety), 2.25 (s, 3H, CH_3), 1.23-1.18 (d, 6H, CH_3 of *p*-cymene moiety); Anal. calc. for ($C_{27}H_{35}N_2O_5ClRuS$): C 50.99, H 5.50, N 4.40, S 5.04; Found: C 51.00, H 5.51, N 4.38, S 5.07; UV-vis (λ_{max}, nm): 229, 269, 382, 426; Mass spectra: *m/z* 635.85 (calcd.), 636.50 (found) [M]$^+$; Color: Dark brown.

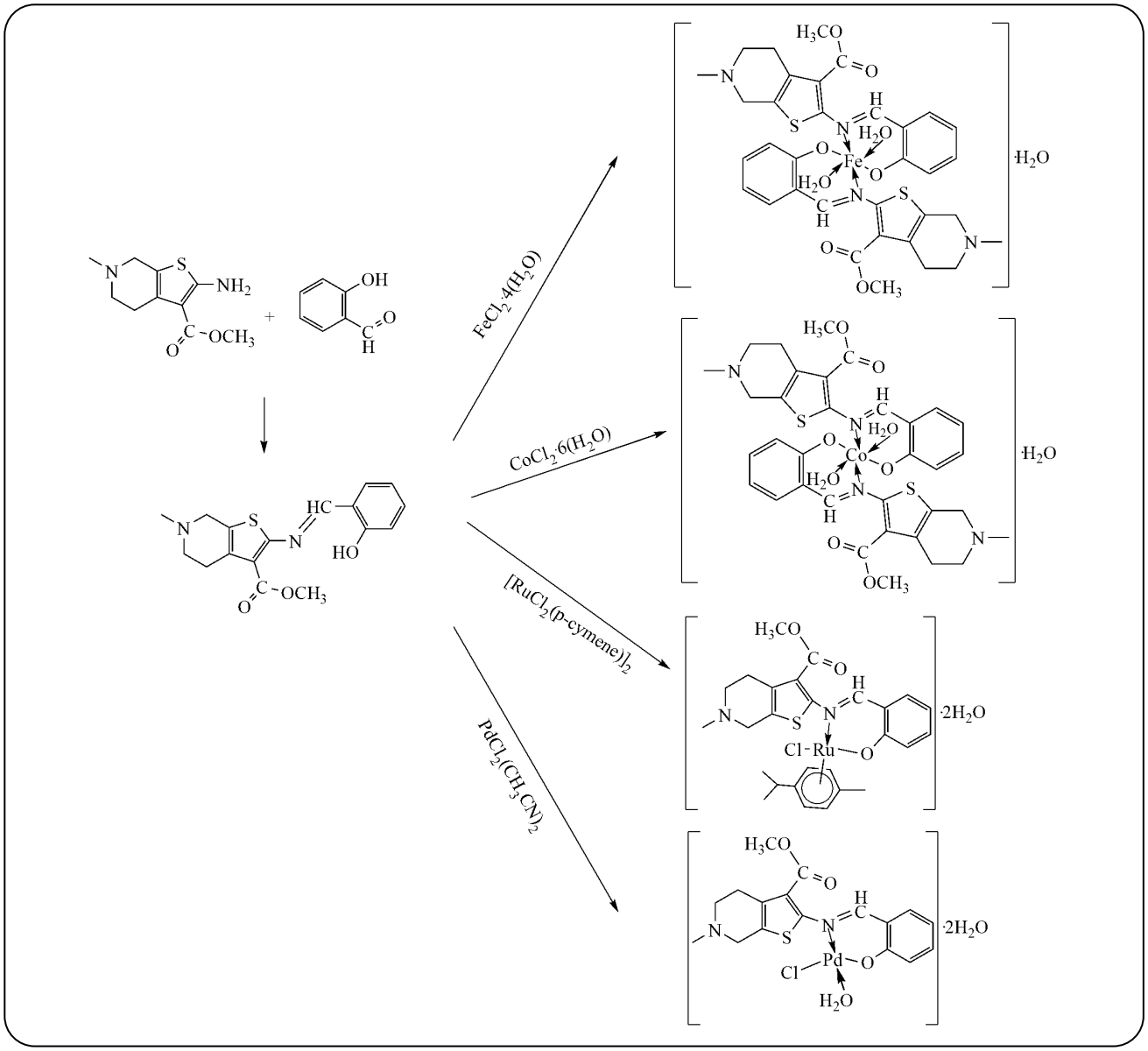

Scheme 1: Synthetic protocol of Schiff base and its metal complexes.

[PdClL(H_2O)]·2H_2O: Yield: 77%; m.p.: 210 °C; FW: 525.10 g/mol; FT-IR (KBr, cm^{-1}): 3506-3429, 3001, 2953, 2869, 1701, 1610, 1571, 1522, 1377, 1200, 751, 550, 501, 457; ^{1}H-NMR (400 Mz, $CDCl_3$, δ, ppm): 8.87 (s, H, CH=N), 7.46-6.99 (m, 4H, Ar.-H), 3.85 (s, 3H, -OC=O-CH_3), 3.71-2.85 (m, 6H, CH_2), 2.51 (s, 3H, N-CH_3); Anal. calc. for ($C_{17}H_{23}N_2O_6PdSCl$): C 38.88, H 4.38, N 5.33, S 6.10; Found: C 39.00, H 3.92, N 5.30, S 6.10; UV-vis (λ_{max}, nm): 212, 279, 309, 457; Mass spectra: *m/z* 525.10 (calcd.), 525.96 (found) $[M]^+$; Color: Light brown.

[$CoL_2(H_2O)_2$]·H_2O: Yield: 87%; m.p.: 280 °C; FW: 771.39 g/mol; FT-IR (KBr, cm^{-1}): 3445-3413, 3051, 2975, 2728, 1701, 1612, 1579-1535, 1378, 1204, 752, 588, 556, 489; Anal. calcd. for ($C_{34}H_{40}CoN_4O_9S_2$): C 52.93, H 5.18, N 7.25, S 8.31. Found: C 52.88, H 5.16, N 7.26, S 8.32; UV-vis (λ_{max}, nm): 212, 322, 480, 502, 608, 673; Mass spectra: *m/z* 771.39 (calcd.), 770.30 (found) $[M+H]^+$; Color: Brick-color.

Antioxidant activities

Total antioxidant capacity

The total antioxidant activity of all compounds was defined according to the method determined by *Mitsuda et al.* [32]. According to this method, the peroxide oxidation

in linoleic acid was metered spectroscopically at 500 nm. The absorbance values of all compounds at 500 nm for every 10 h were measured through the 50 h and the experiment was finished at 40th h when the control sample reached the highest absorbance values. Butylated hydroxyanisole (BHA) and Butylated hydroxytoluene (BHT) were used as standards. The percentages of reduction of peroxidation of compounds and standards were calculated using the following Equation (1):

$$\% \text{ Inhibition} = \left[\left(Abs_0 - Abs_1 \right) / Abs_0 \right] \times 100 \quad (1)$$

Abs₀ and *Abs₁* are the absorbance values of the control and sample, respectively.

Total reduction capability

The capacity of the compounds to reduce Fe^{3+} ions to Fe^{2+} was determined according to the Oyaizu method [33]. The basis of this method is to measure the complexes formed by $K_3Fe(CN)_6$, TCA, and $FeCl_3$ by means of color change in the spectrophotometer at 700 nm. Reagents used were phosphate buffer (0.2 M, pH = 6.6), $K_3Fe(CN)_6$ (1%), TCA solution (10%), $FeCl_3$ (0.1%), BHT (mg/mL), BHA (mg/mL).

The test tubes were mixed and allowed to incubate at 50 °C for 20 minutes. After the incubation, 2.5 mL of 10% TCA solution was added to each test tube brought to room temperature and centrifuged (3000 rpm; 10 min). 2.5 mL of supernatant was transferred to test tubes and 2.5 mL of water was added to the solution followed by 0.5 mL of $FeCl_3$ solution. The blank solution consists of 2.5 mL of TCA, 2.5 mL of deionized water, and 0.5 mL of $FeCl_3$ solution. Finally; dark navy-blue absorbance was measured.

DPPH scavenging effect

The Blois method was used to determine the antiradical properties of the compounds and standard antioxidants [34]. For this purpose, the samples were placed in different concentrations (25µL, 50 µL, and 100 µL). The total volume was then made up to 3 mL with ethyl alcohol. Then 10^{-3} M DPPH radical solution was added to all test tubes and incubated in dark for half-hour. Finally, absorbances were measured at 517 nm against ethanol. The percentage DPPH radical removal activity was calculated using the following equation (2):

$$\text{DPPH scavening activity}(\%) = \left[\left(Abs_0 - Abs_1 \right) / Abs_0 \right] \times 100 \quad (2)$$

Microorganisms and antimicrobial assays

The in vitro antimicrobial activity of the samples and standards was performed by using the hole agar diffusion method. Antimicrobial studies were performed with different Gram-negative (*Escherichia coli* ATCC 11229, *Pseudomonas aeruginosa* ATCC 9027, *Enterobacter aerogenes* ATCC 13048, *Klebsiella pneumoniae* ATCC 13883) and Gram-positive (*Bacillus subtilis* ATCC 6633, *Staphylococcus aureus* ATCC 25923, *Bacillus megaterium* DSM 32 bacteria, fungi (*Yarrowia lipolytica*, *Candida albicans* ATCC 10231, *Saccharomyces cerevisiae*) and antibiotics used in our previous study [34]. All bacteria, fungi, and antibiotics were obtained from the Microbiology laboratory of Muş Alparslan University (Turkey). 25 mg of the compound and standards were dissolved in 1 mL DMSO to form the stock solution. Then, at different concentrations (10 µL, 20 µL, 40 µL, and 80 µL) stock solutions were taken and put into the opened holes. Microorganisms were added to plates and allowed to incubate (24-48 h, 37 ºC).

Investigation of the effects of Schiff base and its M(II) complexes on DNA

The effect of Schiff base and its metal complexes on DNA was determined by the agarose gel electrophoresis method using *p*BR322 plasmid DNA [35]. Compounds were dissolved in DMSO and 20 mg/mL stock solutions were prepared. Intermediate solutions at concentrations of 10, 5, and 2.5 mg/mL were prepared from the stock solutions prepared. Samples were incubated at 37 ºC for 24 h in dark. After incubation, 10 µL of the DNA mixture of the compounds was mixed with a loading buffer. The mixture loaded in 1% agarose gel was applied in 40 V in TBE buffer for 2 h electrophoresis. After electrophoresis, gels were stained with ethidium bromide and photographs were taken in the imaging system [36].

RESULTS AND DISCUSSION

X-ray diffraction analysis

To analyze the structure of the complexes, it was worked with an UltimaIV X- ray diffractometer (Rigaku model, CuK_α=0.1540562 nm). These are the working condition

of XRD measurement; scan step: 0.02°, scanning range: 10-90°, scanning mode: 2Theta/Theta, scanning type: continuous scanning, operating current: 30 mA, operating voltage: 40 kV. XRD results of Co(II), Fe(II), Pd(II), and Ru(II) complexes were given (in Fig. 1 and Fig. 2). Grain sizes of the complexes were calculated with the following Scherer's formula;

$$T = \frac{h\lambda}{W\cos\theta} \quad (3)$$

λ shows X-ray wavelength, θ shows Bragg's diffraction angle, h=0.94 shows constant, W shows full width of half maximum intensity. Average grain sizes (T) of the complexes were calculated from the detected highest peak intensity. Crystal parameters of these complexes were shown in Table 1 and Table 2.

XRD analysis of Co(II) complex

Fig. 1 was the XRD measurement result of Co(II) complex. As it was observed from this figure, XRD showed a wide bump behavior. This was the scattering of the X-ray in all directions. This result proved the Co(II) complex had in the amorphous phase.

XRD analysis of Fe(II) complex

Fig. 2 provided the XRD result of Fe(II) complex. As it can be seen from this figure, an intense peak at 25.6° (intensity 221 (a.u)) was obtained. No other peak was observed. The complex was produced for the first time, so the orientation of the observed peak cannot be given. By using formula 3, we had the grain size of the complex. Table 2 provided the grain size of the complex. The grain size of Fe(II) complex was 13.05 nm.

XRD analysis of Pd(II) complex

Fig. 2 was the XRD measurement result of Pd(II) complex. As detected from this figure, XRD showed a wide bump behavior. This was the scattering of the X-ray in all directions. This result proved the Pd(II) complex had in the amorphous phase.

XRD analysis of Ru(II) complex

In Fig. 2, the XRD measurement result of Ru(II) complex can be seen. We had 4 distinct peaks, which were at 11.5° (intensity 270 a.u), 14.6° (intensity 304 a.u), 16.3° (intensity 232 a.u), and 18.6° (intensity 178.5). Our complex had in polycrystalline nature as proved from the XRD result. By using formula 3, we had the grain sizes of the complex. Table 3 provided the grain sizes of the complex. The highest grain size was found at 11.5° diffraction angle, while the lowest grain size was found at 18.6° diffraction angle.

Table 1: Grain sizes of the Fe(II) complex.

Full Width Half Maximum (W) (°)	2θ (°)	Grain Size (T)(nm)
0.64	25.6	13.05

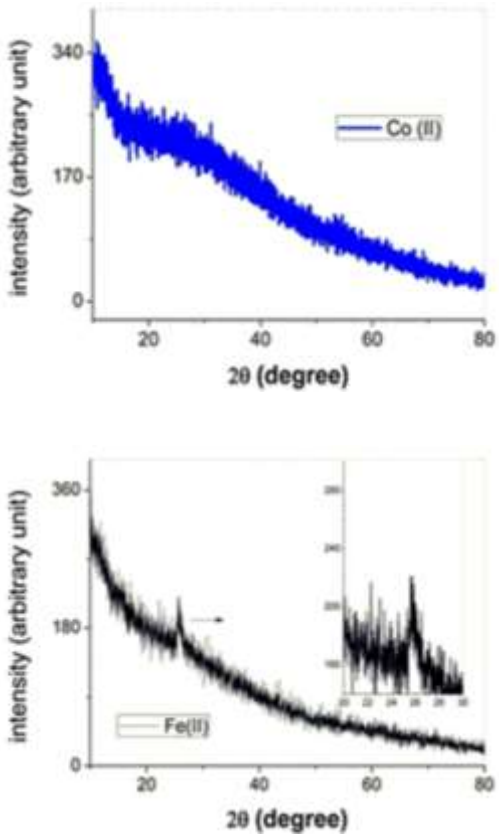

Fig. 1: X-ray diffraction patterns of Co(II) and Fe(II) complexes.

The complex was produced for the first time and the structural properties of similar complexes can be given in References [35,37].

Spectroscopic characterization

Characteristic FT-IR data of Schiff base ligand and its Co(II), Fe(II), Ru(II), Pd(II) complexes were given in the experimental part. All complexes, large and broad peaks in the range 3555-3413 cm^{-1}, were attributable to the coordinated water molecules. The broad bands at 3434

Table 2: Grain sizes of the Ru(II) complex.

Full Width Half Maximum (W) (°)	2θ (°)	Grain Size (T)(nm)
0.04	11.5	207.5
0.49	14.6	16.9
0.54	16.3	15.4
0.58	18.6	14.3

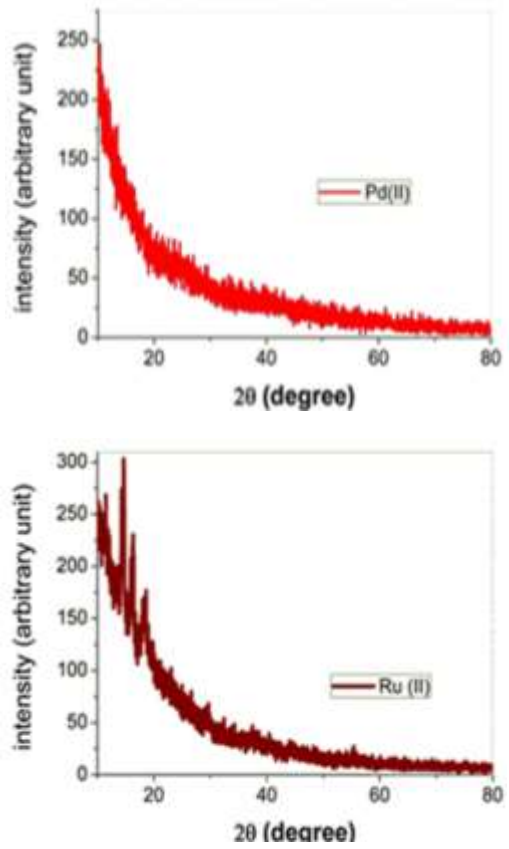

Fig. 2: X-ray diffraction patterns of Pd(II) and Ru(II) complexes.

and 3385 cm^{-1} in the ligand indicated the phenolic hydroxyl group. These bands were not observed in the complexes. This showed that the hydroxyl group was involved in coordination with the oxygen atom. The hydroxyl group attached to the benzene ring of salicylaldehyde was observed at a peak of 1221 cm^{-1}. The values of the hydroxyl group in the complexes showed lower frequency at 1207-1200 cm^{-1} respectively, which was indicating that there was coordination between the metal ion and the oxygen atoms of the (C–O) group. The ligand also observed at 1601 cm^{-1} distinct signal was assigned to the azomethine (CH=N) group. In the spectrum of complexes, the vibrations of the azomethine group were shifted to the higher region of 1612-1609 cm^{-1}. These shifts confirm that the nitrogen atom belonging azomethine group was coordinated with metal ions. 588-501 cm^{-1} and 491-457 cm^{-1} the bands in the range of (M–O) and (M–N) showed vibrations respectively [21,30,35,37]. Also, the IR spectra of Fe(II) and Co(II), and Pd(II) complexes that showed a wide absorption band around 3555-3413 cm^{-1} may be stretching vibrations of (OH) of water molecules associated with the complex [38,39].

Electronic spectra and magnetic measurements were made to determine the geometries of the complexes. All complexes exhibited three intense absorptions at 205-530 nm. The absorption spectra of Co(II), Fe(II), Pd(II), and Ru(II) complexes, dense bands around 205-269 nm and 309-386 nm indicated $\pi \rightarrow \pi^*$ and $n \rightarrow \pi^*$ transitions of the azomethine chromophore, respectively. By comparing the spectra of the ligand and its complexes the absorptions above 420 nm (e.g., 426, 439, 457, 480 nm) were indicated to the ligand to Metal Charge Transfer Transitions (MLCT). The electronic spectra for Pd(II) complex 457 nm indicated a square planar structure around the palladium ion. The electronic spectra for Ru(II)-*p*-cymene complex were similar to this observed in other octahedral half-sandwich Ru(II) complexes. Fe(II) and Co(II) complexes exhibited absorption bands at 520, 530, 608, and 640-678 nm, which attributed to $^2A_{1g} \rightarrow {}^2T_{1g}$, and $^4T_{1g} \rightarrow {}^4T_{2g}$ transitions. The observed magnetic moments for Co(II) and Fe(II) complexes were 4.72 B.M and 4.90 B.M respectively. This might be confirmed in their octahedral geometry [40-44].

Thermal analysis

Thermogravimetric (TG) studies for complexes were conducted from room temperature to 50 to 1000 °C. Decay pressures, temperature ranges, decomposition products, and percentages of mass loss found and calculated for all complexes are shown in Table 3. Thermograms of complexes, starting from 50 °C, the first decomposition products were seen to remove from the molecular water. Depending on the increase in temperature, fragmentation products were seen in up to five steps. Thermal decomposition data for each stage of degradation were given in Table 3 and a general diagram. Thermal decomposition had been proposed with the correlation between the corresponding % weight losses and different weathering steps [1,37].

Table 3: TGA data of Co(II), Fe(II), Pd(II) and Ru(II) complex compounds.

Complexes	Decomp. stages	The temperature range in TG (°C)	Wt. loss (mg) Calcd. (Found)		Decomp. assignment
$[FeL_2(H_2O)_2]\cdot H_2O$	1	50-130	2.34	2.69	H_2O
	2	130-290	23.18	23.54	$2H_2O$, $C_8H_{18}N_2$
	3	290-485	18.10	18.14	$C_6H_3O_2S$
	4	485-760	17.32	17.32	$C_7H_5ON_2$
	5	760-900	29.69	29.55	$C_{13}H_8O_2S$
	Residue				FeO
$[PdClL(H_2O)]\cdot 2H_2O$	1	50-140	6.85	6.82	$2H_2O$
	2	140-280	10.18	10.15	H_2O, Cl
	3	280-420	16.95	16.92	C_7H_5
	4	420-650	13.52	13.49	C_4H_9N
	5	650-900	15.50	15.49	$C_6H_3O_2NS$
	Residue				PdO
[RuCl(*p*-cymene)L]·$2H_2O$	1	50-150	5.66	5.64	$2H_2O$
	2	150-270	26.66	26.64	$C_{10}H_{14}Cl$
	3	270-460	32.41	32.37	$C_{12}H_{16}O_2N$
	4	460-900	16.83	16.80	C_5HNS
	Residue				RuO
$[CoL_2(H_2O)_2]\cdot H_2O$	1	50-150	2.33	2.69	H_2O,
	2	165-250	14.66	14.10	$2H_2O$, $C_3H_9O_2$
	3	250-380	16.47	15.98	$C_7H_{15}N_2$
	4	380-540	33.99	33.84	$C_{17}H_{10}O_3$
	5	540-900	22.83	22.56	$C_7N_2S_2$
	Residue				CoO

Total antioxidant activity results

The determination of antioxidant activities of ligand and its complexes was done by the ferric thiocyanate method. When the activity results measured at different concentrations were examined, it was found that activities generally increased depending on the concentration (Fig. 3). According to the results; The percentage removal of linoleic acid peroxidation of the compound and standards at a concentration of 100 µL occurred in the following order: BHT (81.75%), Fe(II) complex (80.09%), BHA (78.51%), Co(II) complex (78.46%), L (78.37%), Ru(II) complex (78.29%), and Pd(II) complex (21.23%).

The results showed that the Fe(II) complex had the best activity and that other ligand and metal complexes had similar activity to the standards. In previous studies investigating the antioxidant properties of Schiff base and metal complexes, it was reported that metal complexes increase the activity of ligands [45-48]. In our previous study, we observed that Ru(II) and Co(II) complexes inhibited lipid peroxides to a close degree to standard BHA and BHT antioxidants [35]. In the current study, the Co(II) and Ru(II) complexes exhibited activity close to the standards (BHA and BHT) and this supported previous studies.

Reducing power results

The capacity of ligand and its metal complexes and standards to reduce iron ions generally increased due to an increase in their concentration. According to the results,

the iron ions reduction power of the compounds was realized in the following order (Fig. 4): BHA > BHT > Co(II) complex > Pd(II) complex > Fe(II) complex > L > Ru(II) complex.

When we looked at the results, standards have the highest reduction capacities, followed by Co(II) and Pd(II) complexes. In our previous study, we found that the Fe^{3+} reduction capacity of the Fe(II) complex performed better activity than the Schiff base ligand and the present study supported these results [46].

Antiradical activity

The antiradical properties of the ligand and its metal complexes and standard antioxidants were examined by looking at the sweep effects on DPPH radicals. The basis of this method is based on measuring the absorbance change by neutralizing the DPPH radical with antioxidants [49]. DPPH radical scavenging percentage of the samples (100 µL) were performed, respectively, as follows (Fig. 5): BHA (82.30%) > Ru(II) complex (64.30%) > BHT (52.50%) > Co(II) complex (36.80%) > Fe(II) complex (27.90%) > Pd(II) complex (11.60%) > L (9.10%). In the previous study, it was reported that Ru(II) and Pd(II) complexes exhibited DPPH radical scavenging activity close to standard ascorbic acid [49]. Another study reported that the Ru(II) complex performed better than standard ascorbic acid [27]. The current study, especially Ru(II) complex supported the previous studies by showing better radical removal activity than BHT used as the standard.

Antimicrobial activity

To compare the antimicrobial activity of the ligand and its metal complexes were tested against *E. aerogenes*, *E. coli*, *P. aeruginosa*, *K. pneumoniae*, *B. subtilis*, *S. aureus*, *B. megaterium*, *Y. lipolytica*, *C. albicans*, and *S. cerevisiae*. The observed antimicrobial and standard antibiotic inhibition zone values (mm) were summarized in Tables 4-6.

The *in vitro* antimicrobial activities of the ligand and its metal complexes at 10 µL, 20 µL, 40 µL, and 80 µL aliquots were tested against ten microorganisms. The present results showed that the ligand and its metal complexes exhibited a broad antimicrobial activity producing 12-36 mm inhibition zones. The highest antimicrobial activity was demonstrated against the Co(II) complex *P. aeroginosa* (36±2.0 mm) while the lowest antimicrobial activity was detected against the Fe(II)

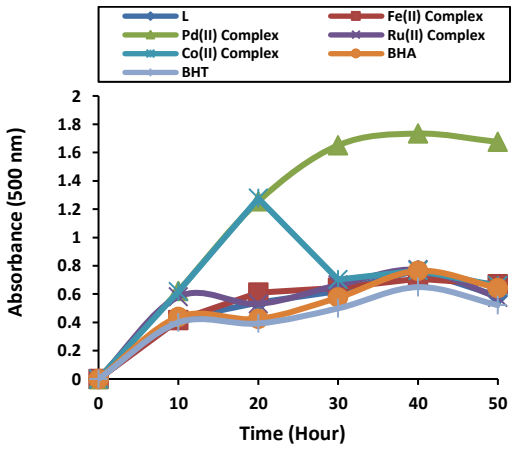

Fig. 3: The total antioxidant activity of the ligand, its complexes, and standard antioxidants (BHA and BHT).

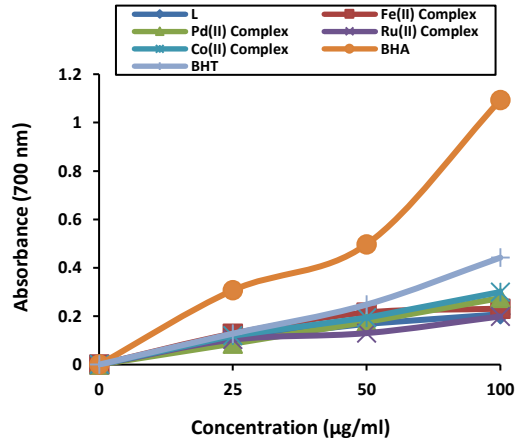

Fig. 4: Reducing the power of the ligand, metal complexes, and standard antioxidants using Fe^{3+}-Fe^{2+}.

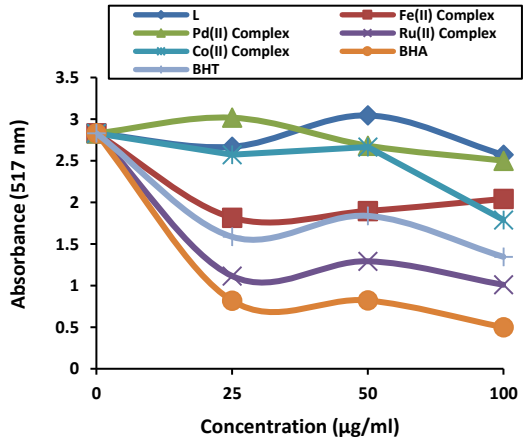

Fig. 5: DPPH free radical scavenging activity of ligand, its metal complexes, and standard antioxidants (BHA and BHT).

Table 4: Effect of Schiff base ligand and antibiotic discs on test microorganisms.

Microorganisms		Ligand				Antibiotics				
		10 µl	20 µl	40 µl	80 µl	E-15	SAM-20	AK-30	RD-5	FCA-25
Gram Positive	*B. subtilis*	N/A	N/A	13±0.0	17±0.6	20±0.0	14±1.0	11±1.0	21±0.0	N/A
	S. aureus	N/A	N/A	13±0.0	16±0.0	21±1.0	10±0.0	9±0.0	18±1.0	N/A
	B. megaterium	N/A	12±0.0	13±0.0	18±0.0	25±0.0	N/A	10±1.0	16±0.0	N/A
Gram Negative	*E. aerogenes*	N/A	12±0.0	14±0.0	18±0.6	27±1.0	10±1.0	9±0.0	16±1.0	N/A
	E. coli	N/A	N/A	13±0.6	17±0.0	19±1.5	13±0.0	13±0.0	18±0.0	N/A
	P.aeroginosa	N/A	N/A	14±0.0	18±0.6	19±0.0	N/A	14±1.0	8±0.0	N/A
	K. pneumonia	12±0.0	13±0.0	15±0.6	18±1.0	19±1.7	16±0.6	10±0.0	19±1.5	N/A
Fungus	*Y.lipolytica*	N/A	13±0.0	14±0.0	17±0.0	N/A	N/A	N/A	N/A	21±0.0
	C.albicans	N/A	N/A	15±0.0	16±0.6	N/A	N/A	N/A	N/A	23±1.5
	S. cereviciae	N/A	N/A	N/A	14±0.0	N/A	N/A	N/A	N/A	N/A

Table 5: Effect of Co(II) and Ru(II) complex compounds on test microorganisms.

Microorganisms		L+Co(II)				L+ Ru(II)			
		10 µl	20 µl	40 µl	80 µl	10 µl	20 µl	40 µl	80 µl
Gram Positive	*B. subtilis*	16±1.0	20±0.6	27±1.0	30±1.5	16±0.0	20±2.0	23±1.0	26±1.5
	S. aureus	N/A	N/A	N/A	N/A	17±0.6	20±0.6	24±2.0	27±1.0
	B. megaterium	16±0.6	21±1.0	25±0.0	28±0.6	16±1.0	19±1.0	22±1.5	25±0.6
Gram Negative	*E. aerogenes*	16±1.0	21±0.6	26±1.0	30±1.0	15±0.6	19±2.0	22±0.6	24±2.0
	E. coli	16±0.0	22±1.0	27±0.6	30±1.5	16±1.0	18±1.0	21±2.0	24±1.5
	P. aeroginosa	23±0.0	27±1.5	33±2.0	36±2.0	15±0.0	18±0.6	24±1.0	27±2.0
	K. pneumonia	18±0.6	23±1.0	28±0.0	30±0.6	17±1.0	20±2.0	23±0.6	25±1.0
Fungus	*Y. lipolytica*	N/A	14±0.6	18±0.0	22±1.0	N/A	12±0.0	14±1.0	16±0.6
	C. albicans	N/A	14±0.0	19±1.0	25±2.0	N/A	13±0.0	15±0.6	18±2.0
	S. cereviciae	N/A	12±0.0	16±0.6	20±1.0	N/A	13±0.0	15±0.0	17±1.0

N/A: No Available

complex *P. aeroginosa*. Antimicrobial activity was increased due to increased concentrations of ligands and complexes. The Fe(II) complex exhibited antimicrobial activity, such as partial ligand. When the antimicrobial effects of the ligand and its metal complexes were compared, it was seen that metal complexes were more effective on microorganisms than ligand (Tables 4-6).

The antibacterial activities of the ligand and its metal complexes were also compared with the reference antibiotics. As seen in Table 4, ligand and metal complexes, except for the ligand, exhibited better activity than standard antibiotics.

N/A: No Available, Erythromycin (E-15), Ampicillin/Sulbactam(SAM-20), Amikacin (AK30), Rifampicin (RD-5), Fluconazole (FCA-25)

Antimicrobial activity criteria are based on inhibition zone diameter (mm). They show significant activity when the zone diameter is more than 20 mm [50,51]. When all of the compounds, except ligand, were evaluated in general, they showed significant antimicrobial activity by creating an inhibition zone of more than 20 mm. The metal complexes have been found to show good antimicrobial activity by creating a larger 13 mm diameter inhibition

Table 6. Effect of the Pd(II) and Fe(II) complex compounds on test microorganisms.

Microorganisms		L+Pd(II)				L+ Fe(II)			
		10 µl	20 µl	40 µl	80 µl	10 µl	20 µl	40 µl	80 µl
Gram Positive	*B. subtilis*	18±0.6	20±1.0	24±0.6	28±0.6	N/A	12±0.0	20±1.0	25±0.6
	S. aureus	21±1.0	25±2.0	28±1.0	30±2.0	N/A	N/A	17±0.0	22±1.0
	B. megaterium	16±0.6	20±0.0	24±0.6	28±1.5	N/A	12±0.0	17±0.6	22±0.0
Gram Negative	*E. aerogenes*	20±1.0	23±1.5	25±2.0	28±1.0	N/A	13±0.0	16±0.0	22±1.5
	E. coli	20±1.0	24±1.0	28±1.5	29±2.0	12±0.0	16±0.6	25±1.0	28±0.6
	P. aeroginosa	20±1.0	25±1.0	28±2.0	30±1.5	12±0.0	15±0.0	20±0.6	25±1.0
	K. pneumonia	19±0.6	24±0.6	27±1.5	30±0.6	N/A	12±0.0	15±0.0	23±0.0
Fungus	*Y. lipolytica*	13±0.0	18±0.6	23±1.0	30±1.0	N/A	N/A	20±1.0	30±2.0
	C. albicans	13±0.0	16±0.6	20±0.6	27±1.5	N/A	N/A	16±0.6	22±1.0
	S. cereviciae	N/A	13±0.0	15±1.0	22±0.6	N/A	N/A	N/A	12±0.0

N/A: No Available

zone against bacteria and fungi [52]. The ligand and its metal complexes showed good antimicrobial activity by showing a high concentration (80 µL) of 14-36 mm inhibition zone. The ligand did not show activity against S. aureus, while complexes were found to show good activity. Except for the Co(II) complex, other compounds were found to show good antibacterial activity against S. aureus. The Schiff base ligand showed good antibacterial and antifungal activity against test organisms [53]. In studies of the antimicrobial activities of ligands and their metal complexes, it is observed that most metal chelates showed higher antibacterial activity than free ligands [54]. Such increasing activity of metal chelates can be explained on the basis of Overtone's concept [55] and Tweedy's theory of chelation [56]. In the study, it was determined that metal complexes showed high antimicrobial activity. Results were supported by the literature.

DNA cleavage studies

The DNA protective activity of the ligand and its Co(II), Fe(II), Pd(II), Ru(II) complexes was examined used by *p*BR322 plasmid DNA (Fig. 6). The effect of different molarities of ligands and their complexes on DNA damage in the presence of H_2O_2 and DMSO, the factors causing DNA damage, were assessed according to this method.

According to the image obtained, it was observed that H_2O_2 fragmented Form I and completely destroyed DNA with DMSO (Fig. 6). DMSO had no effect on DNA alone. It was found that when only the Fe(II) complex was applied, it completely destroyed the DNA, while the Fe(II) complex stabilized plasmid DNA by removing and scavenging the effect of H_2O_2 + DMSO. In addition, when Co(II) complex was applied at low concentration alone, it was determined that it did not eliminate the scavenging effect of H_2O_2 + DMSO while leaving the plasmid DNA in a stable state. It was seen that Ru(II) and Pd(II) complexes did not eliminate the scavenging effect of H_2O_2 + DMSO and they eliminated DNA once they were applied alone (Fig. 6).

In *Iftikhar et al.* study, Cu(II) complex of the Schiff base caused great damage to plasmid DNA at all concentrations [1]. In another study, they found that the metal complexes degraded plasmid DNA in a better ratio [57]. It was determined that the ligand and Ru(II) complex can convert DNA from Form I to Form II [25]. In our study, metal complexes have similar damage to plasmid DNA as in the literature.

CONCLUSIONS

The ligand containing salicylaldehyde and its four new metal complexes were synthesized. The structures of these compounds were determined by various spectroscopic techniques. All spectroscopic results showed that Co(II), Fe(II), and Ru(*p*-cymene) complexes had the octahedral geometry and the Pd(II) complex had the square plane. And then in vitro, antioxidant, antimicrobial, antifungal activities and DNA cleavage studies of Schiff base ligand

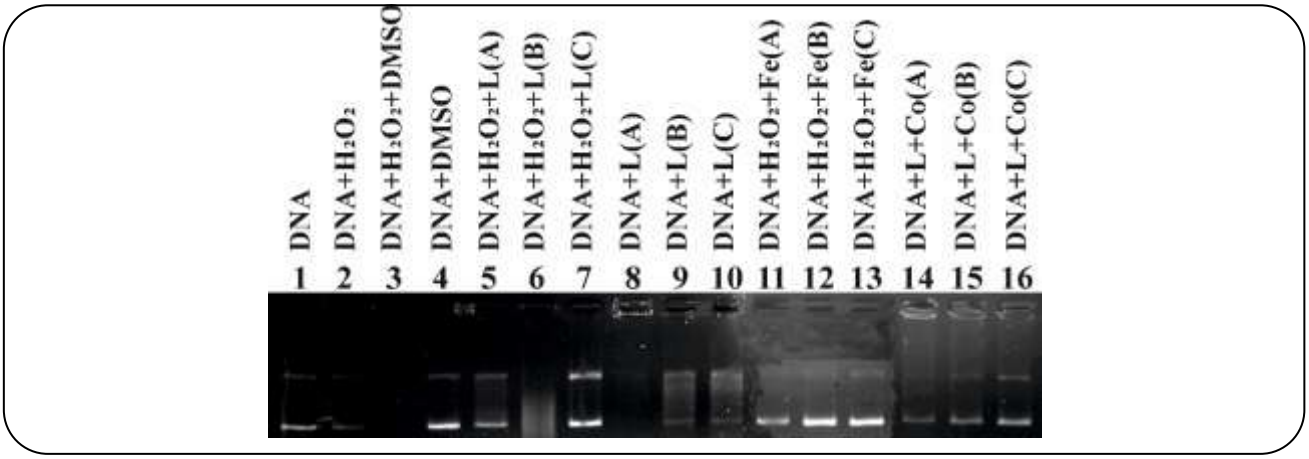

Fig. 6: The DNA protective activity of the ligand and its complexes A (10 mg/mL), B (5 mg/mL) and C (2.5 mg/mL).

and complexes were evaluated. When the results of the study was evaluated, it was seen that both ligand and its metal complexes generally exhibited good antioxidant activity. When metal complexes were compared, it was found that Fe(II) and Co(II) complexes showed the best antioxidant effect and Pd(II) complexes showed the lowest antioxidant effect. When the antimicrobial activities of all synthesized compounds were examined, it was found that especially metal complexes showed better activity than ligands. Among the metal complexes, it was observed that the best microbial activity was exhibited by the Co(II) metal complex. Metal complexes exhibited better antifungal activity than ligands. DNA cleavage studies of the complexes show that the Fe(II) complex can effectively cleave plasmid DNA in the existence of an oxidizing agent H_2O_2. In addition, among the complexes, Fe(II) complex was found to exhibit good antimicrobial, DNA binding, and cleavage properties.

Acknowledgment

We thank the Scientific Research-Publications and Projects Research and Practice Center (BAYPUAM) under research project no MŞÜ16-TMY-G01 for their support.

Received : Jun. 4, 2021 ; Accepted : Oct. 10, 2021

REFERENCES

[1] Iftikhar B., Javed K., Khan M.S.U., Akhter Z., Mirza B., Mckee V., Synthesis, Characterization and Biological Assay of Salicylaldehyde Schiff Base Cu(II) Complexes and Their Precursors, *J. Mol. Struct.*, **1155**: 337-348 (2018).

[2] Yang J., Shi R., Zhou P., Qiu Q., Li H., Asymmetric Schiff Bases Derived from Diaminomaleonitrile and Their Metal Complexes, *J. Mol. Struct.*, **1106**: 242-258 (2016).

[3] Liu X., Manzur C., Novoa N., Celedón S., Carrillo D., Hamon J.R., Multi Dentate Unsymmetrically-Substituted Schiff Bases and Their Metal Complexes: Synthesis, Functional Materials Properties, and Applications to Catalysis, *Coord. Chem. Rev.*, **357**: 144-172 (2018).

[4] Zakerhamidi M.S., Nejati K., Sorkhabi S.G., Saati M., Substituent and Solvent Effects on the Spectroscopic Properties and Dipole Moments of Hydroxylbenzaldehyde Azo Dye and Related Schiff Bases, *J. Mol. Liq.*, **180**: 225-234 (2013).

[5] Arroudj S., Bouchouit M., Bouchouit K., Bouraiou A., Messaadia L., Kulyk B., Figa V., Bouacida S., Sofiani Z., Taboukhat S., Synthesis, Spectral, Optical Properties and Theoretical Calculations on Schiff Bases Ligands Containing *o*-Tolidine, *Op. Mater.*, **56**: 116-120 (2016).

[6] Satheesh C.E., Kumar P.R., Sharma P., Lingaraju K., Palakshamurthy B.S., Naika H.R., Synthesis, Characterization and Antimicrobial Activity of New Palladium and Nickel Complexes Containing Schiff Bases, *Inorg. Chim. Acta*, **442**: 1-9 (2016).

[7] Deilami A.B., Salehi M., Arab A., Amiri A., Synthesis, Crystal Structure, Electrochemical Properties and DFT Calculations of Three New Zn(II), Ni(II) and Co(III) Complexes Based on 5-Bromo-2-((allylimino)methyl)phenol Schiff-Based Ligand, *Inorg. Chim. Acta*, **476**: 93-100 (2018).

[8] Tan Y-X., Zhang Z-J., Liu Y., Yu J-X., Zhu X-M., Kuang D-Z., Jiang WJ., Synthesis, Crystal Structure and Biological Activity of the Schiff Base Organotin(IV) Complexes Based on Salicylaldehyde-*o*-aminophenol, *J. Mol. Struct.*, **1149**: 874-881 (2017).

[9] Yang J., Shi R., Zhou P., Qiu Q., Li H., Asymmetric Schiff Bases Derived from Diamino Malenitrile and Their Metal Complexes, *J. Mol. Struct.*, **1106**: 242-258 (2016).

[10] Zaltariov M.F., Avadanei M., Balan M., Peptanariu D., Vornicu N., Shova S., Synthesis, Structural Characterization and Biological Studies of New Schiff Bases Containing Trimethylsilyl Groups, *J. Mol. Struct.*, **1175**: 624-631 (2019).

[11] Sumrra S.H., Habiba U., Zafar W., Imran M., Chohan Z.H., A Review on the Efficacy and Medicinal Applications of Metal-Based Triazole Derivatives, *J. Coord. Chem.*, **73**: 2838-2877 (2020).

[12] Buldurun K., Turan N., Aras A., Mantarcı A., Turkan F., Bursal E., Spectroscopic and Structural Characterization, Enzyme Inhibitions, and Antioxidant Effects of New Ru(II) and Ni(II) Complexes of Schiff Base, *Chem. Biodivers.*, **16(8)**: e1900243 (2019).

[13] Araújo E.L., Hellen de F.G.B., Dockal E.R., Cavalheiro É.T.G., Synthesis, Characterization and Biological Activity of Cu(II), Ni(II) and Zn(II) Complexes of Biopolymeric Schiff Bases of Salicylaldehydes and Chitosan, *Int. J. Biol. Macromol.*, **95**: 168-176 (2017).

[14] Parsaee Z., Mohammadi K., Synthesis, Characterization, Nano-Sized Binuclear Nickel Complexes, DFT Calculations and Antibacterial Evaluation of New Macrocyclic Schiff Base Compounds, *J. Mol. Struct.*, **1137**: 512-523 (2017).

[15] Szady-Chełmieniecka A., Kołodziej B., Morawiak M., Kamieński B., Schiff W., Spectroscopic Studies of the Intramolecular Hydrogen Bonding in *o*-Hydroxy Schiff Bases, Derived from Diamino Maleonitrile, and Their Deprotonation Reaction Products, *Spectrochim. Acta, Part A*, **189**: 330-341 (2018).

[16] Buldurun K., Turan K., Bursal E., Aras A., Mantarcı A., Çolak N., Türkan F. Gülçin İ., Synthesis, Characterization, Powder X-Ray Diffraction Analysis, Thermal Stability, Antioxidant Properties and Enzyme Inhibitions of M(II)-Schiff Base Ligand Complexes, *J. Biomol. Struct. Dyn.*, **39**: 6480-6487 (2021).

[17] Ceyhan G., Çelik C., Urus S., Demirtaş I., Elmastaş M., Tümer M., Antioxidant, Electrochemical, Thermal, Antimicrobial and Alkane Oxidation Properties of Tridentate Schiff Base Ligands and Their Metal Complexes, *Spectrochim. Acta, Part A*, **81**: 184-198 (2011).

[18] Tadavi S.K., Yadav A.A., Bendre R.S., Synthesis and Characterization of A Novel Schiff Base of 1,2-Diamino Propane with Substituted Salicyaldehyde and Its Transition Metal Complexes: Single Crystal Structures and Biological Activities, *J. Mol. Struct.*, **1152**: 223-231 (2018).

[19] Taha Z.A., Hijazi A.K., Ababneh T.S., Mhaidat I., Ajlouni A.M., Al-Hassan K.A., Mitzithra C., Hamilakis S., Danladi F., Altalafha A.Y., Photophysical Properties and Computational Study of Newly Synthesized Lanthanide Complexes with N-(2-Carboxyphenyl) Salicylideneimine Schiff Base Ligand, *J. Lumin.*, **18**: 230-239 (2017).

[20] Özdemir Ö., Novel Symmetric Diimine-Schiff Bases and Asymmetric Triimine-Schiff Bases as Chemo Sensors for the Detection of Various Metal Ions, *J. Mol. Struct.*, **1125**: 260-271 (2016).

[21] Pervaiz M., Ahmad I., Yousaf M., Kirn S., Munawar A., Saeed Z., Adnan A., Gulzar T., Kamal T., Ahmad A., Rashid A., Synthesis, Spectral and Antimicrobial Studies of Amino Acid Derivative Schiff Base Metal (Co, Mn, Cu and Cd) Complexes, *Spectrochim. Acta, Part A*, **206**: 642-649 (2019).

[22] Patil S.A., Unki S.N., Kulkarni A.D., Naik V.H., Badami P.S., Co(II), Ni(II) and Cu(II) Complexes with Coumarin-8-yl Schiff-Bases: Spectroscopic, in Vitro Antimicrobial, DNA Cleavage and Fluorescence Studies, *Spectrochim. Acta, Part A*, **79**: 1128-1136 (2011).

[23] Khalid S., Sumrra S.H., Chohan Z.H., Isatin Endowed Metal Chelates as Antibacterial and Antifungal Agents, *Sains Malays.*, **49**: 1891-1904 (2020).

[24] Bursal E., Turkan F., Buldurun K., Turan N., Aras A., Çolak N., Murahari M., Yergeri M.C., Transition Metal Complexes of A Multidentate Schiff Base Ligand Containing Pyridine: Synthesis, Characterization, Enzyme Inhibitions, Antioxidant Properties, and Molecular Docking Studies, *Biometals*, **34**: 393-406 (2021).

[25] Nair M.S., Arish D., Joseyphus R.S., Synthesis, Characterization, Antifungal, Antibacterial and DNA Cleavage Studies of Some Heterocyclic Schiff Base Metal Complexes, *J. Saudi. Chem. Soc.*, **16**: 83-88 (2012).

[26] Turan N., Adigüzel R., Buldurun K., Bursal E., Spectroscopic, Thermal and Antioxidant Properties of Novel Mixed Ligand-Metal Complexes Obtained from Saccharinate Complexes and Azo Dye Ligand (Mnppa), *Int. J. Pharmacol.*, **12**: 92-100 (2016).

[27] Gaber M., El-Ghamry H.A., Fathalla S.K., Ni(II), Pd(II) and Pt(II) Complexes of (1H-1,2,4-triazole-3-ylimino)methyl]naphthalene-2-ol. Structural, Spectroscopic, Biological, Cytotoxicity, Antioxidant and DNA Binding, *Spectrochim. Acta, Part A*, **139**: 396-404 (2015).

[28] Sumrra S., Hanif M., Chohan Z.H., Design, Synthesis and in Vitro Bactericidal/Fungicidal Screening of Some Vanadyl (IV) Complexes with Mono-and Di-Substituted ONS Donor Triazoles, *J. Enzyme Inhib. Med. Chem.*, **30**: 800-808 (2015).

[29] Ali M.A., Mirza A.H., Ting W.Y., Hamid M.H.S.A., Bernhardt P.V., Butcher R.J., Mixed-Ligand Nickel(II) and Copper(II) Complexes of Tridentate ONS and NNS Ligands Derived from S-Alkyldithiocarbazates with the Saccharination as a Co-Ligand, *Polyhedron*, **48**: 167-173 (2012).

[30] Daravath S., Kumar M.P., Rambabu A., Vamsikrishna N., Shivaraj N.G., Design, Synthesis, Spectral Characterization, DNA Interaction and Biological Activity Studies of Copper(II), Cobalt(II) and Nickel(II) Complexes of 6-Amino Benzothiazole Derivatives, J. Mol. Struct., **1144**: 147-158 (2017).

[31] Turan N., Buldurun K., Gündüz B., Çolak N., Synthesis and Structures of Fe(II), Zn(II) and Pd(II) Complexes with A Schiff Base Derived from Methyl 2-Amino-6-methyl-4,5,6,7-tetrahydrothieno[2,3-*c*] pyridine-3-carboxylate and Comparison of Their Optical Constants for Different Solvents and Molarities, *J. Nanoelectron. Optoelectron.*, **12**: 1028-1040 (2017).

[32] Pandiarajan D., Ramesh R., Ruthenium(II) Half-Sandwich Complexes Containing Thioamides: Synthesis, Structures and Catalytic Transfer Hydrogenation of Ketones, *J. Organomet. Chem.*, **723**: 26-35 (2013).

[33] Kilic A., Savci A., Alan Y., Beyazsakal L., The Synthesis of Novel Boronate Esters and N-Heterocyclic Carbene (NHC)-Stabilized Boronate Esters: Spectroscopy, Antimicrobial and Antioxidant Studies, *J. Organomet. Chem.*, **917**: 121268 (2020).

[34] Blois M.S., Antioxidant Determinations by the Use of a Stable Free Radical, *Nature*, **26**: 1199-1200 (1958).

[35] Turan N., Buldurun K., Alan Y., Savci A., Çolak N., Mantarci A., Synthesis, Characterization, Antioxidant, Antimicrobial and DNA Binding Properties of Ruthenium(II), Cobalt(II) and Nickel(II) Complexes of Schiff Base Containing *o*-Vanillin, *Res. Chem. Intermediat.*, **45**: 3525-3540 (2019).

[36] Londershausen M., Approaches to New Parasiticides, Pestic. Sci., **48**(4): 269-292 (1996).

[37] Gönül İ., Synthesis and Structural Characterization of ONO Type Tridentate Ligands and Their Co(II) and Ni(II) Complexes: Investigation of Electrical Conductivity and Antioxidant Properties, *Inorg. Chim. Acta*, **495**: 1-8 (2019).

[38] Buldurun K., Turan N., Savcı A., Çolak N., Synthesis, Structural Characterization and Biological Activities of Metal(II) Complexes with Schiff Bases Derived from 5-Bromosalicylaldehyde: Ru(II) Complexes Transfer Hydrogenation, *J. Saudi. Chem. Soc.*, **23**: 205-214 (2019).

[39] Yeğiner G., Gülcan M., Işık S., Ürüt G.Ö., Özdemir S., Kurtoğlu M., Transition Metal(II) Complexes with A Novel Azo-Azomethine Schiff Base Ligand: Synthesis, Structural and Spectroscopic Characterization, Thermal Properties and Biological Applications, *J. Fluoresc.*, **27**: 2239-2251 (2017).

[40] Çalık H.S., Ispir I, Karabuga S., Aslantaş M., Ruthenium(II) Complexes of NO Ligands: Synthesis, Characterization and Application in Transfer Hydrogenation of Carbonyl Compounds, *J. Organomet. Chem.*, **801**: 122-129 (2016).

[41] Ramesh M., Vetkatachalam G., Half-Sandwich (H_6-*p*-Cymene) Ruthenium(II) Complexes Bearing 5-Amino-1-methyl-3-phenylpyrazole Schiff Base Ligands: Synthesis, Structure and Catalytic Transfer Hydrogenation of Ketones, *J. Organomet. Chem.*, **880**: 47-55 (2019).

[42] Ekennia A.C., Osowole A.A., Olasunkanmi L.O., Onwudiwe D.C., Olubiyi O.O., Ebenso E.E., Synthesis, Characterization, DFT Calculations and Molecular Docking Studies of Metal(II) Complexes, *J. Mol. Struct.*, **1150**: 279-292 (2017).

[43] Sathishkumar P.N., Raveendran N., Bhuvanesh N.S.P., Karwembu R., Chemoselective Transfer Hydrogenation of Nitroarenes, Ketones and Aldehydes Using Acylthiourea Based Ru(II)(*p*-Cymene) Complexes as Precatalysts, *J. Organomet. Chem.*, **876**: 57-65 (2018).

[44] Turan N., Buldurun K., Çolak N., Özdemir İ., Preparation and Spectroscopic Studies of Fe(II), Ru(II), Pd(II) and Zn(II) Complexes of Schiff Base Containing Terephthalaldehyde and Their Transfer Hydrogenation and Suzuki-Miyaura Coupling Reaction, *Open. Chem.*, **17**: 571-580 (2019).

[45] Turan N., Savci A., Buldurun K., Alan Y., Adigüzel R., Synthesis and Chemical Structure Elucidation of Two Schiff Base Ligands, Their Iron(II) and Zinc(II) Complexes, and Antiradical, Antimicrobial, Antioxidant Properties, *Lett. Org. Chem.*, **13**: 343-351 (2016).

[46] More M.S., Joshi P.G., Mishra Y.K., Khanna P.K., Metal Complexes Driven from Schiff Bases and Semicarbazones for Biomedical and Allied Applications: A Review, *Mater. Today Chem*., **14**: 100195 (2019).

[47] Ünver Y., Deniz S., Çelik F., Akar Z., Küçük M., Sancak K., Synthesis of New 1,2,4-Triazole Compounds Containing Schiff and Mannich Bases (Morpholine) with Antioxidant and Antimicrobial Activities, *J. Enzyme. Inhib. Med. Chem.*, **31**: 89-95 (2016).

[48] Aboafia S.A., Elsayed S.A., El-Sayed A.K.A., El-Hendawy A.M., New Transition Metal Complexes of 2,4-Dihydroxybenzaldehyde Benzoylhydrazone Schiff Base (H_2dhbh): Synthesis, Spectroscopic Characterization, DNA Binding/Cleavage and Antioxidant Activity, *J. Mol. Struct.*, **1158**: 39-50 (2018).

[49] Devagi G., Dallemer F., Kalaivani P., Prabhakaran R., Organometallic Ruthenium(II) Complexes Containing NS Donor Schiff Bases: Synthesis, Structure, Electrochemistry, DNA/BSA Binding, DNA Cleavage, Radical Scavenging and Antibacterial Activities, *J. Organomet. Chem*., **854**: 1-14 (2018).

[50] Hellas C.M.Y., Chan H.L., Yang M., Determination of Mode of Interactions Between Novel Drugs and Calf Thymus DNA by Using Quartz Crystal Resonator, *Sensors Actuat. B*, **81**: 283-288 (2002).

[51] Rehman A., Choudhary M.I., Thomsen W.J., "Bioassay Techniques for Drug Development", Harwood Academic Publishers, Amsterdam, The Netherlands, pp. 9, (2001).

[52] Shungu D.L., Weinberg E., Cerami A.T., Evaluation of Three Broth Disk Methods for Testing the Susceptibility of Anaerobic Bacteria to Imipenem, *J. Clin. Microbiol.*, **21**: 875-879 (1985).

[53] Bakirdere E.G., Fellah M.F., Canpolat E., Kaya M., Synthesis and Characterization of A New 2-{(*E*)-[(4-aminophenyl)imino]methyl}-6-bromo-4-chlorophenol and Its Complexes with Co(II), Ni(II), Cu(II), and Zn(II): An Experimental and DFT Study, *Synth. React. Inorg. Metal-Org. Nano-Metal Chem.*, **45**: 1337 (2015).

[54] Amjad M., Sumrra S.H., Akram M.S., Chohan Z.H., Metal-Based Ethanolamine-Derived Compounds: A Note on Their Synthesis, Characterization and Bioactivity, J. *Enzyme Inhib. Med. Chem.*, **31**: 88-97 (2016).

[55] Dharamaraj N., Viswanathamurthi P., Natarajan K., Ruthenium (II) Complexes Contain Bidentate Schiff Bases and Their Antifungal Activity, *Trans. Met. Chem.*, **26**: 105-109 (2001).

[56] Anacona J.R., Rodriguez A., Synthesis and Antibacterial Activity of Ceftriaxone Metal Complexes, *Trans. Met. Chem.*, **30**: 897 (2005).

[57] Venkateswarlu K., Kumar M.P., Rambabu A., Vamsikrishna N., Daravath S., Rangan K., Crystal Structure, DNA Binding, Cleavage, Antioxidant and Antibacterial Studies of Cu(II), Ni(II) and Co(III) Complexes with 2-((Furan-2-yl)methylimino)methyl)-6-ethoxyphenol Schiff Base, *J. Mol. Struct.*, **1160**: 198-207 (2018).